Relative strength of thermal and electrical spin currents in a ferromagnetic tunnel contact on a semiconductor

K.-R. Jeon, H. Saito, S. Yuasa, and R. Jansen

National Institute of Advanced Industrial Science and Technology (AIST), Spintronics Research Center, Tsukuba, Ibaraki 305–8568, Japan

The relative magnitude of electrical and thermal spin currents is investigated for a ferromagnetic tunnel contact on a semiconductor. A direct quantitative comparison is made by simultaneously generating electrical and thermal spin currents of opposite sign and determining the compensation point at which the sum of both spin currents vanishes. This avoids the need to determine the magnitude of each spin current. Surprisingly, it is found that in a $Co_{70}Fe_{30}/MgO/Si$ tunnel contact, the thermal spin current driven by a temperature difference of less than 1 K across the contact is comparable to the electrical spin current induced by a bias voltage of about 22 mV. This suggests that the thermal generation of spin current is more efficient than hitherto assumed and should be considered in the design and analysis of spintronic devices that use spin current or spin transfer torque.

I. INTRODUCTION

The efficient generation of spin current, the flow of spin angular momentum, is indispensable in spintronics, in which digital information is represented by the orientation of spins. It has been well established that spin currents can be created by a spin-polarized charge current, via spin-orbit interaction, or by magnetization dynamics [1–5]. Interestingly, heat flow and thermal gradients have recently also been used to drive spin currents in various ferromagnetic nanostructures, including magnetic tunnel contacts [6–20]. It is an important goal to understand what controls the magnitude of the thermal spin current and to understand how large it is. This is not only relevant in itself, but also because other (nonthermal) methods to create spin currents involve driving forces (charge current, magnetization dynamics) that dissipate energy and thus simultaneously induce heat flow and temperature gradients. The resulting thermal spin currents need to be distinguished from the intended nonthermal spin current.

From a technological perspective, an important question asks what is the efficiency of the generation of a thermal spin current and, in particular, what is the efficiency compared to other methods to create spin current. As a point of reference, one may use spin currents that are induced by sending a (spin-polarized) charge current through a ferromagnetic tunnel contact since this technologically viable means of achieving a sizable spin polarization [1–4] is widely used and the method has been rather well optimized during a period of four decades since the first demonstration of spin-polarized tunneling [21]. The thermal analogue of spin-polarized tunneling is Seebeck spin tunneling (SST), which enables the generation of a spin current across a ferromagnetic tunnel contact by a temperature difference between the two electrodes [9]. The spin current is a pure spin current, i.e., it exists without a charge tunnel current. This thermal spin current has been shown to arise from the spin-dependent Seebeck coefficient, $S^{\uparrow} - S^{\downarrow}$, of a tunnel contact with a ferromagnetic electrode [22,23], with $S^{\uparrow}$ and $S^{\downarrow}$ being the Seebeck coefficient for majority spins ($\uparrow$) and minority spins ($\downarrow$), respectively. Although SST was discovered only a few years ago [9] and is far from being optimized, it is of interest to compare the magnitude of the spin currents in tunnel junctions created by thermal and electrical driving forces.

There is a fundamental difference in the ultimate limits of electrical and thermal spin currents. The spin current that accompanies an electrical charge current has an upper bound because the current spin polarization cannot be larger than 100% (fully polarized charge current). However, this limitation does not exist for thermal spin currents. That is, the spin-dependent Seebeck coefficient $S^{\uparrow} - S^{\downarrow}$ that controls the thermal spin current can certainly be larger than the charge Seebeck coefficient S_0. Indeed, in a recent experiment [20], it was found that $S^{\uparrow} - S^{\downarrow}$ of the Heusler alloy CoFeAl is about three times larger than S_0. Another recent study [24] revealed that for a magnetic tunnel junction (MTJ), a temperature difference of 1 K across an MgO tunnel barrier generates giant thermal spin torques equivalent to the electrical spin transfer torque that would be created by a bias voltage of about 25 mV. Although more work is certainly needed, these experiments seem to suggest that thermal spin currents are more pronounced than thus far assumed.

Here, we experimentally compare the relative strength of electrical and thermal spin currents in a ferromagnetic tunnel contact on a semiconductor. Electrical and thermal spin currents with opposite signs are simultaneously generated across a single tunnel contact, and then the compensation point, at which the sum of both spin currents vanishes, is determined. This enables us to make a direct quantitative comparison. It avoids the need to determine the actual value of the spin currents and eliminates factors common to both, such as those associated with the conversion of the spin current into a detectable (spin voltage) signal. Strikingly, it is found that in a $Co_{70}Fe_{30}/MgO/Si$ junction, the thermal spin current driven by a temperature difference of less than 1 K across the tunnel contact is comparable to the electrical spin current induced by a voltage of about 22 mV. The efficiency of thermal spin injection is thus unexpectedly large, suggesting that thermal spin currents can be of significance in spintronic devices.

II. EXPERIMENTAL DETAILS

A magnetic tunnel contact consisting of a 5.0-nm-thick ferromagnetic $Co_{70}Fe_{30}$ electrode and a 1.5-nm-thick MgO tunnel barrier with (001)-texture structure was prepared on a silicon on insulator (SOI) wafer by molecular beam epitaxy
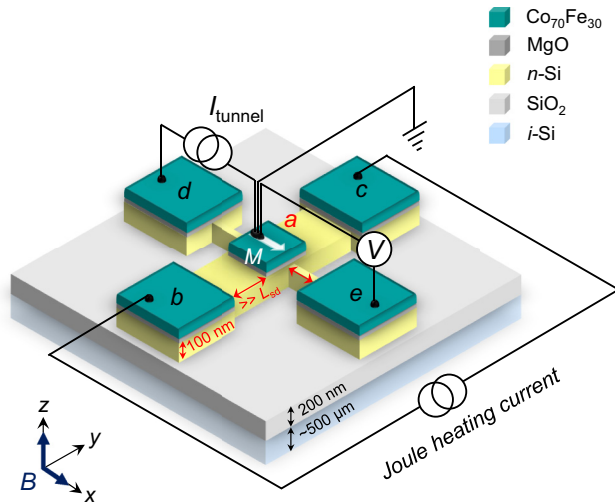
FIG. 1. (Color online) Sketch of the device layout and the electrical connections used to induce and probe spin currents in the central $Co_{70}Fe_{30}/MgO/Si$ tunnel contact.

under optimized growth conditions, as described previously [25]. The n-type SOI wafer has a Si device layer that is (001)-oriented and phosphorus doped with a carrier density of $\sim 10^{19}\,cm^{-3}$ at 300 K. The thickness of the Si device layer is only 100 nm. This confines the Joule heating current in the Si to a region close to the MgO tunnel contact while also simplifying the calculation of the temperature difference across the contact.

The device layout is depicted in Fig. 1. It allows the simultaneous generation of the electrical and thermal spin current in the central active tunnel contact (a) that has a size of $40 \times 50\,\mu m^2$. The Si channel has lateral dimensions of $50 \times 400\,\mu m^2$ and is connected via side arms to four identical reference contacts (b, c, d, and e) of $150 \times 150\,\mu m^2$ that are used to generate and probe the spin currents, as described below. The Si channel and the contacts are defined by standard photolithography and Ar-ion beam etching. The active contact (a) is separated by more than $150\,\mu m$ from the reference contacts, which is much larger than the spin-diffusion length. On a single piece of wafer there are several independent tunnel devices.

The measurement procedure is as follows. A charge tunnel current (I_{tunnel}) can be induced across the active tunnel contact using another contact (d) as a reference. This induces an electrical spin current that is linearly proportional to I_{tunnel}. Simultaneously, yet independently, a thermal bias across the active tunnel contact can be established by sending a Joule heating current ($I_{heating}$) through the Si channel using two reference contacts (b) and (c) at opposite ends of the Si channel. This raises the temperature (T_{Si}) of the Si with respect to the temperature (T_{CoFe}) of the $Co_{70}Fe_{30}$ ferromagnet and causes a heat flow from the Si to the ferromagnet across the central tunnel contact. The corresponding thermal spin current is quadratic in $I_{heating}$.

To probe the spin currents, the voltage across the central tunnel contact is measured using contact (e) as a reference. The total voltage measured is given by $V = V_0 + \Delta V_{TH} + \Delta V_{EL}$. The first term V_0 is a (spin-independent) background voltage that includes any charge thermovoltage created. The second

and third terms are spin voltages that are proportional to the spin accumulation (usually parameterized by the spin splitting $\Delta\mu$ of the electrochemical potential) that is created by the thermal (ΔV_{TH}) or electrical (ΔV_{EL}) driving force, respectively. The latter two contributions can be detected by means of the Hanle [26–28] and inverted Hanle [29] effects. These are obtained, respectively, when an external magnetic field is applied perpendicular (B_z) or parallel (B_x) to the orientation of the accumulated spins, causing the suppression of the spin accumulation as a consequence of spin precession (Hanle effect) or the recovery of $\Delta\mu$ (inverted Hanle effect). This results in a detectable voltage change (ΔV) that is proportional to the nonequilibrium spin population and thus to the spin current [26–29].

III. RESULTS

A. Compensation of thermal and electrical spin currents

Let us start by describing the simultaneous generation of thermal and electrical spin currents of opposite signs and the determination of the compensation point at which the sum of both spin currents vanishes. In Fig. 2(a), the spin signals due to the Hanle effect (closed symbols) and the inverted Hanle effect (open symbols) are presented for a $Co_{70}Fe_{30}/MgO/Si$ tunnel contact subjected to different combinations of electrical and thermal driving forces. When only a thermal driving force is present (top panels, $I_{heating}$ is nonzero, $I_{tunnel} = 0$), the spin signals have the same sign regardless of the polarity of the heating current. This is consistent with a thermally induced spin current, as in previous reports on SST across a ferromagnetic tunnel contact [9–12]. The total Hanle signal, as given by the sum of the Hanle and inverted Hanle signals [29], is positive for the direction of the heat flow used.

In order to achieve a compensation of spin currents, we then add an electrical spin current that creates a spin signal of the opposite sign. The middle and bottom panels of Fig. 2(a) depict the corresponding Hanle and inverted Hanle signals, obtained by adding a negative bias current ($I_{tunnel} < 0$) across the same tunnel contact. Indeed, the spin signal is negative when only the electrical driving force is present ($I_{heating} = 0$). When a thermal as well as an electrical driving force is present, the sign and magnitude of the resulting spin voltage depends on the relative magnitude of the electrical and thermal spin signals. Notably, one can observe that the net spin signal vanishes at certain combinations of the heating current and tunnel current. For example, for $I_{heating} = 1.75\,mA$, the spin signal vanishes when $I_{tunnel} = -0.1\,mA$, whereas for $I_{heating} = 3.0\,mA$, the spin signal vanishes if a larger tunnel current of $I_{tunnel} = -0.4\,mA$ is applied. These results demonstrate that one can indeed create a situation in which the electrical and thermal spin currents of opposite signs cancel each other and the total spin current vanishes. The bias voltage at which this compensation occurs will be referred to as the compensation point.

In order to assure that a genuine compensation of electrical and thermal spin currents occurs, one needs to measure the full Hanle response curve. This includes not only the low field part that is presented in Fig. 2(a) but also the features at larger magnetic field that are characteristic of the presence of nonequilibrium spin accumulation in the tunnel contact [29,30]. The result is shown in Fig. 2(b). The middle and bottom panels
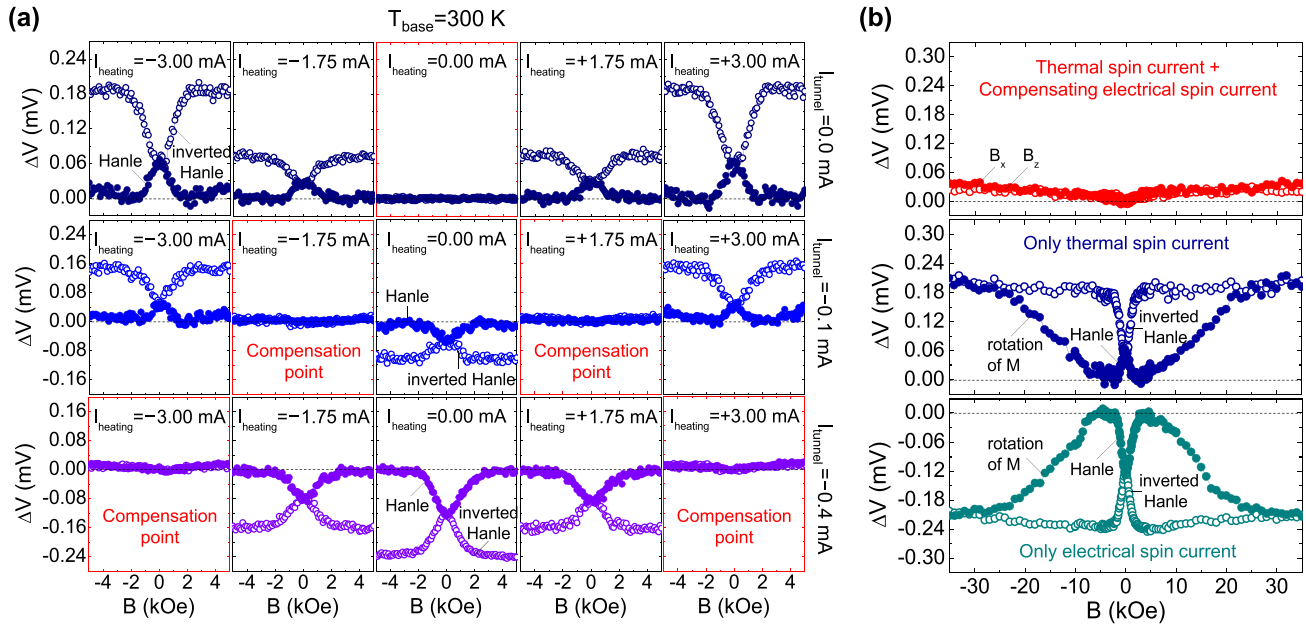
FIG. 2. (Color online) (a) Obtained spin signals (ΔV) are shown for heating currents ($I_{heating}$) of -3.00, -1.75, 0.00, $+1.75$, and $+3.00$ mA (from left to right), with the bias voltage across the active $Co_{70}Fe_{30}$/MgO/Si tunnel contact fixed by setting the tunnel current (I_{tunnel}) at 0.0, -0.1, and -0.4 mA for the top, middle, and bottom panels, respectively. A negative sign of I_{tunnel} corresponds to electrons tunneling from the Si into the $Co_{70}Fe_{30}$. The solid (open) symbols represent the spin signal from the Hanle (inverted Hanle) effect obtained for an applied magnetic field B_z perpendicular (B_x parallel) to the accumulated spins. All data was measured at a base temperature (T_{base}) of 300 K. (b) The top panel shows spin signals obtained at the compensation point using simultaneous thermal and electrical driving forces ($I_{heating} = +3$ mA, $I_{tunnel} = -0.4$ mA) for applied magnetic fields up to 35 kOe in perpendicular direction (closed circles, Hanle geometry) and in-plane direction (open circles, inverted Hanle geometry). Similar data are shown for a pure thermal driving force (middle panel, $I_{heating} = +3$ mA, $I_{tunnel} = 0.0$) and a pure electrical driving force (bottom panel, $I_{heating} = 0$ mA and $I_{tunnel} = -0.4$ mA).

show the Hanle signals obtained when there is either only an electrical spin current ($I_{tunnel} = -0.4$ mA) or only a thermal spin current ($I_{heating} = +3$ mA). In addition to the low-field part already shown, we observe that there is a pronounced change in the signal for larger perpendicular fields up to about 22 kOe (Hanle geometry). As previously explained [29,30], this is due to the rotation of the magnetization of the ferromagnetic electrode into the direction of the out-of-plane magnetic field. This gradually reduces the angle between the spins and the magnetic field so that the spin precession disappears and the spin accumulation recovers. This additional feature of a nonequilibrium spin accumulation is observed for electrical as well as thermal driving forces. In fact, for both cases the shape of the curve is similar, and the magnitude of the spin signals is also identical except for the sign. Consequently, at the compensation point [Fig. 2(b), top panel] there is only a small residual signal, and none of the features characteristic of the Hanle effect is observed for magnetic fields up to 35 kOe. This proves that the spin accumulation has really disappeared and that the net spin current vanishes at the compensation point.

B. Relative strength of thermal and electrical spin currents

From the compensation point, one can determine the relative strength of thermal and electrical spin currents. First, the bias voltage required to achieve compensation is determined for different values of the thermal driving force. The magnitude of the Hanle spin signal was extracted from

curves, such as shown in Fig. 2(a), and plotted as a function of heating current and tunnel current across the contact [see Fig. 3(a)]. We observe that the signal is quadratic as a function of the heating current and approximately linear as a function of tunnel bias voltage, as expected for the thermally and electrically driven spin current, respectively. From such data, we can extract different combinations of heating current and tunnel bias that result in a compensation point.

The bias voltage (V_{com}) at which compensation is reached is plotted as a function of the heating current in the top panel of Fig. 3(b). We observed that the compensation voltage increases with heating current in an approximately quadratic fashion. This is expected from the scaling of the signals shown in Fig. 3(a) if the thermal spin current itself does not vary strongly when a bias voltage is applied across the tunnel contact. Although it was recently shown that thermal spin signals depend on bias voltage due to the energy dispersion of the tunnel spin polarization [12,31], the variation was found to be very weak for the negative bias voltage at which the compensation point occurs.

Perhaps the most surprising result is the magnitude of the compensation voltage. It reaches values up to 110 mV for the largest heating current used in this experiment. To appreciate this result, we have calculated the temperature difference ($\Delta T = T_{Si} - T_{CoFe}$) across the tunnel contact as a function of $I_{heating}$ [bottom panel of Fig. 3(b)]. As explained in Appendix A, the calculation was performed using the lowest reasonable value (a few times 10^5 Wm^{-2} K^{-1}) of the
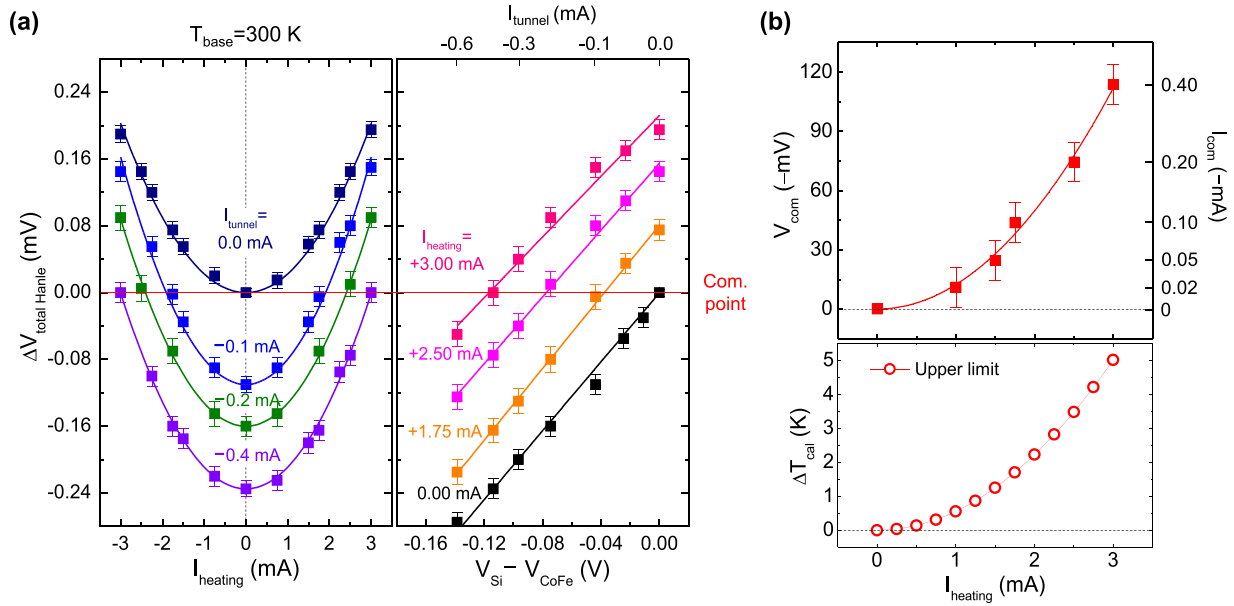
FIG. 3. (Color online) (a) (Left panel) Total spin signals ($\Delta V_{\text{total Hanle}}$ given by the sum of the Hanle and inverted Hanle signals) as a function of the heating current (I_{heating}), with the bias across the tunnel contact set by fixing the tunnel current (I_{tunnel}) at -0.0 (navy symbols), -0.1 (blue), -0.2 (olive), and -0.4 mA (violet), together with fits based on a quadratic scaling (solid lines). (a) (Right panel) The $\Delta V_{\text{total Hanle}}$ as a function of bias voltage, without heating of the Si (black symbols) and with heating (pink, magenta, and orange symbols), together with fits based on a linear scaling (solid lines). (b) Extracted value of the bias voltage (V_{com}) to reach the compensation point (top panel) and calculated temperature difference (ΔT_{cal}) across the tunnel contact (bottom panel), both as a function of the heating current (I_{heating}).

thermal conductance of the 1.5-nm-thick MgO barrier and its interfaces, which means that the calculated value of ΔT should be considered as an upper limit (the actual value of ΔT is likely smaller). Since ΔT as well as the compensation voltage is quadratic as a function of the heating current, we obtain a constant ratio $V_{\text{com}}/\Delta T$ of about 22 mV/K. In other words, a temperature difference of less than 1 K creates a thermal spin current that is comparable to the electrical spin current created by a 22 mV bias voltage.

IV. DISCUSSION

As discussed in Appendices B and C, we do not believe that tunneling via localized states in the tunnel contact, or Hanle signals due to spin heat accumulation, can account for the unexpectedly large thermal spin current. Let us therefore compare the experimental result for the compensation point with what is expected according to the theory for direct tunneling under thermal or electrical bias [23]. For a given temperature difference (ΔT) and electrical current density (J) across the ferromagnetic tunnel contact, the total spin accumulation ($\Delta\mu_{\text{tot}}$) is given by [23]

$$\Delta\mu_{\text{tot}} = \Delta\mu_{\text{TH}} + \Delta\mu_{\text{EL}}$$
$$= \left(\frac{er_s}{R_{\text{tun}}}\right)\lfloor(1 - P_G^2)(S^\uparrow - S^\downarrow)\Delta T + (2P_G)R_{\text{tun}}J\rfloor.$$
(1)

The first term is due to the thermal spin current, and the second is due to the electrical spin current, where e is the electron charge and P_G is the tunnel spin polarization. The tunnel resistance (R_{tun}) of the contact was taken to be much

larger than the spin resistance (r_s) of the semiconductor. Since for the negative bias voltages used here it was found [31] that none of the parameters depend significantly on bias voltage, we can use Eq. (1) to evaluate the compensation point. At the compensation point, the total spin accumulation is zero ($\Delta\mu_{\text{tot}} = 0$), so that we can exclude the prefactor that contains the conversion of spin current into spin accumulation. Setting the term between straight brackets to zero and noting that the factors $(1 - P_G^2)$ and $(2P_G)$ are of order unity for typical values of P_G of $0.5 - 0.7$ for crystalline Co$_{70}$Fe$_{30}$/MgO tunnel contacts [32,33], we deduce that at the compensation point, the ratio of the voltage $R_{\text{tun}}J$ and ΔT should be comparable to $(S^\uparrow - S^\downarrow)$. Hence, in order to explain the experimental result (>22 mV/K, see the previous section) the spin-dependent Seebeck coefficient ($S^\uparrow - S^\downarrow$) of the tunnel contact would need to have a comparable value.

To put this into perspective, the charge Seebeck coefficient S_0 of a nonmagnetic tunnel junction has been calculated to be in the range of $50-100\,\mu$V/K using free electron models [34,35]. Recent experiments [24] on MgO-based tunnel junctions with reliable temperature calibration yielded charge Seebeck coefficients of about $30\,\mu$V/K at 10 K, while *ab initio* calculations based on coherent tunneling predicted charge Seebeck coefficients around $30\,\mu$V/K at room temperature for Fe-MgO-Fe tunnel junctions [36]. Thus, if indeed $S^\uparrow - S^\downarrow$ is of the order of 22 mV/K, it implies that it is more than two orders of magnitude larger than the charge Seebeck coefficient. As stated in the Introduction, it is certainly possible that $S^\uparrow - S^\downarrow$ is larger than the charge Seebeck coefficient S_0 for a ferromagnetic tunnel contact, although explicit confirmations are so far scarce. A ratio of a factor of two or three can be derived from calculations for Fe-MgO-Fe tunnel junctions
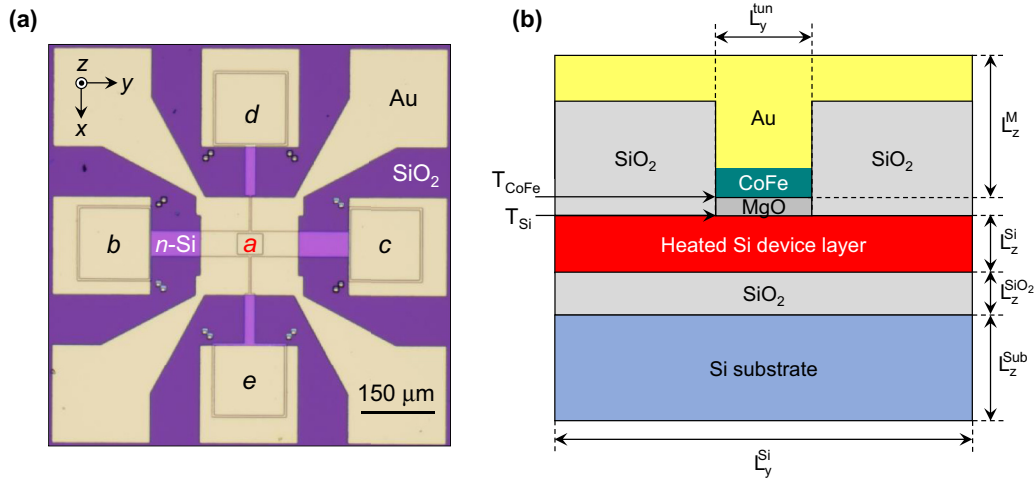
FIG. 4. (Color online) (a) Optical microscope image of the fabricated device with a central active tunnel contact of $40 \times 50 \, \mu m^2$, and (b) schematic of its vertical structure (not to scale) used for the calculation of the temperature difference ($\Delta T \equiv T_{Si} - T_{CoFe}$) that develops across the MgO tunnel barrier when the Si device layer is heated by a Joule heating current.

[36], whereas a factor of three was measured for a thermally driven transport in a CoFeAl alloy [20]. Nevertheless, whether the spin-dependent Seebeck coefficient can be two or more orders of magnitude larger than the charge Seebeck coefficient is unclear.

Our results indicate that to obtain thermal and electrical spin currents of equal magnitude, the required driving force is much smaller for the thermal spin current (for the latter, the driving force $S_0 \Delta T < 50 \, \mu V$ assuming $S_0 \approx 50 \, \mu V/K$, whereas the driving force is about 22 mV for the compensating electrical spin current). Interestingly, a similar conclusion can be drawn from recent experiments [24] on thermal spin transfer torque in MgO-based MTJs, in which driving forces $S_0 \Delta T$ of about $60 \, \mu V$ induced thermal torques of a magnitude equivalent to that of the electrical spin transfer torque created by a driving force (bias voltage) of the order of 25 mV. Although at present we have no detailed explanation for these puzzling results, a natural starting point for further work is to examine aspects that are not included in the present theories for electrical and thermal spin current generation. These aspects include deviations from equilibrium near the tunnel interfaces, contributions from inelastic (phonon or magnon-assisted) tunneling, or spin currents and torques due to collective magnetic excitations.

V. CONCLUSIONS

We investigated the relative magnitude of electrical and thermal spin currents in a ferromagnetic tunnel contact on a semiconductor. A direct comparison is enabled by exploiting the compensation point, at which the sum of the simultaneously generated electrical and thermal spin currents with opposite sign vanishes. Strikingly, it is found that in a $Co_{70}Fe_{30}$/MgO/Si tunnel contact, the thermal spin current driven by a temperature difference of less than 1 K across the contact is comparable to the electrical spin current induced by a bias voltage of about 22 mV. This suggests that the thermal creation of spin current is more efficient than hitherto assumed and needs to be considered in the design and analysis of spintronic devices that utilize spin current or spin transfer torque.

APPENDIX A: CALCULATION OF THE TEMPERATURE DIFFERENCE ACROSS THE TUNNEL BARRIER

In order to calculate the temperature difference ($\Delta T \equiv T_{Si} - T_{CoFe}$) across the MgO tunnel barrier, we consider the device structure depicted in Fig. 4 and follow the procedure described previously in the supplement of Ref. [9]. The ΔT is obtained from a one-dimensional (1D) heat flow model with a geometric correction that accounts for lateral heat transport in the Si layer towards the tunnel contact area. The ΔT is expressed as [9]

$$\Delta T \equiv T_{Si} - T_{CoFe} = \left(\frac{P_{heating} L_z^{Si}}{G_{th}^{tun}} \right) R_Q F, \quad (A1)$$

$$R_Q = \frac{\alpha^{**}}{1 + (\alpha/G_{th}^{tun}) + (\alpha/\alpha^M)}, \quad (A2)$$

$$1 \leqslant F \leqslant \left(\frac{L_x^{Si} L_y^{Si}}{L_x^{tun} L_y^{tun}} \right). \quad (A3)$$

Here, G_{th}^{tun} is the thermal conductance of tunnel barrier, and $P_{heating}$ is the power density associated with the Joule heating in the Si that equals $\rho_{Si} J_{heating}^2$, where ρ_{Si} is the resistivity of the Si layer and $J_{heating}$ is the heating current density. $L_{x,y,z}^{Si}$ and $L_{x,y,z}^{tun}$ denote the dimensions of the Si layer and the tunnel barrier, respectively. The factor R_Q describes the fraction

TABLE I. Material parameters and their values used in the calculation of the temperature difference across the tunnel barrier: the thickness (L_z^i), the thermal conductivity (k^i), and the thermal conductance (α^i) for each layer, together with some derived quantities.

Material	$L_z^i [\mu m]$	$k^i [W\,m^{-1}\,K^{-1}]$	$\alpha^i [W\,m^{-2}\,K^{-1}]$
Si (substrate)	$L_z^{sub} = 500$	$k^{sub} = 150$	$\alpha^{sub} = 3 \times 10^5$
SiO$_2$	$L_z^{SiO_2} = 0.2$	$k^{SiO_2} = 1.4$	$\alpha^{SiO_2} = 7 \times 10^6$
n-Si (device layer)	$L_z^{Si} = 0.1$	$k^{Si} = 150$	$\alpha^{Si} = 1.5 \times 10^9$
Au (metal)	$L_z^M = 0.2$	$k^M = 318$	$\alpha^M = 1.59 \times 10^9$

$\alpha^* = \frac{\alpha^{sub}\alpha^{SiO_2}}{\alpha^{sub}+\alpha^{SiO_2}} = 2.88 \times 10^5\,W\,m^{-2}\,K^{-1}, \quad \alpha = \frac{\alpha^*\alpha^{Si}}{\alpha^*+\alpha^{Si}} = 2.88 \times 10^5\,W\,m^{-2}\,K^{-1}, \quad \alpha^{**} = \frac{\alpha^*+2\alpha^{Si}}{2(\alpha^*+\alpha^{Si})} = 1, \quad \frac{L_x^{Si}L_y^{Si}}{L_x^{tun}L_y^{tun}} = 10$

of the Joule heat produced in the Si device layer that flows through the tunnel barrier, whereas $\alpha^i = k^i/L_z^i$ is the thermal conductance for each layer, given by the ratio of the thermal conductivity k^i and the thickness of the layer, with values and some derived parameters that are defined in Table I. Finally, F is the geometric correction factor that takes account of lateral heat flow within the Si layer towards the tunnel contact (note that F has a maximum value of 10 given by the ratio of the lateral dimensions of the Si strip $50 \times 400\,\mu m^2$ and the tunnel contact $40 \times 50\,\mu m^2$).

The calculated ΔT values as a function of the thermal conductance G_{th}^{tun} of the tunnel barrier are shown in Fig. 5 for the purely 1D case ($F = 1$) and the three-dimensional (3D) case with maximum lateral heat flow ($F = 10$). The calculation was done for the maximum heating power $P_{heating} = 13.5\,\mu W\,\mu m^{-3}$, which is obtained at the maximum heater current (3 mA). As previously noted [9], the calculated value of ΔT depends significantly on the value of G_{th}^{tun}, and this constitutes the main uncertainty in estimating the value of ΔT. The thermal conductivity (k^{MgO}) of a thin MgO film depends

on its thickness as well as its crystal structure [37,38], and also the thermal resistance of the MgO/Si and Co$_{70}$Fe$_{30}$/MgO interfaces should be taken into account. For a polycrystalline MgO film with a grain size of $3 \sim 7$ nm, a thermal conductance of $2.5 \times 10^7\,Wm^{-2}\,K^{-1}$ was determined at room temperature [38]. However, for the ultrathin layers used here, the interfaces are expected to limit the thermal conductance due to phonon scattering. Considering all this, we estimate the upper limit of ΔT by taking a rather low value of a few times $10^5\,Wm^{-2}\,K^{-1}$ (dashed line in Fig. 5) and a value of $F = 2$ for the geometric correction. This finally leads to an upper limit of $\Delta T = 5\,K$ obtained at the maximum Joule heating current.

APPENDIX B: DISCUSSION OF SPIN HEAT ACCUMULATION

It was recently predicted that a spin heat accumulation [39], i.e., a difference in the temperature of electrons with different spin orientation, can also develop in a magnetic tunnel contact on a semiconductor and produce a voltage signal in a Hanle measurement [40]. We therefore discuss whether this can affect the ratio of the observed Hanle spin signals under thermal and electrical driving forces. Let us first assume that the spin heat currents dominate the Hanle signals. Then, at the compensation point where the sum of the thermally and electrically induced spin heat current vanishes and the net spin heat accumulation is zero, the ratio of $R_{tun}J$ and ΔT is given [40] by $(P_k^{el}\frac{L_0}{S_0^2} - P_L)S_0/P_L$. Here, P_L is the spin polarization of thermoelectric conductance, P_k^{el} is the spin polarization of electronic heat conductance that is expected [40] to be equal to the electron tunnel spin polarization (P_G), and L_0 is the Lorentz number ($2.45 \times 10^{-8}\,V^2\,K^{-2}$). For reasonable parameters ($P_k^{el} = P_G = 0.7$, $S_0 = 20\,\mu V/K$, and $P_L = 0.04$), one can obtain a ratio of $R_{tun}J/\Delta T = 21\,mV/K$ that is very close to the experimentally observed ratio (see the end of Sec. III B). Hence, the spin heat current can easily be dominated by the thermally driven component and requires relatively small driving force in comparison to spin heat current driven electrically. Yet, it would seem unlikely that this can explain the experimental result because it would require that the observed Hanle signals are dominated by the spin heat accumulation rather than the spin accumulation. As discussed previously [40], this does not seem to be a very plausible situation because in general one would expect the spin heat accumulation to relax faster than the spin accumulation.
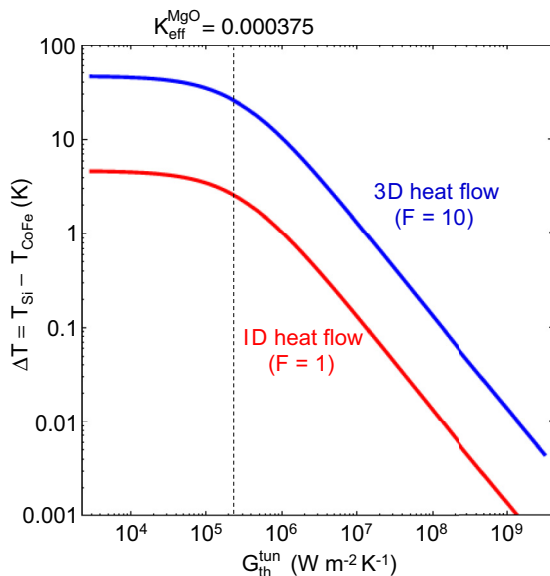
FIG. 5. (Color online) Calculated values of the temperature difference ($\Delta T \equiv T_{Si} - T_{CoFe}$) as a function of the thermal conductance (G_{th}^{tun}) of the tunnel barrier at the maximum Joule heating power ($P_{heating}$) of $13.5\,\mu W\,\mu m^{-3}$ applied to the Si device layer. The red curve corresponds to the case of 1D heat flow ($F = 1$), and the blue curve is for the case of 3D heat flow with the maximum lateral heat flow ($F = 10$).

APPENDIX C: DISCUSSION OF TUNNELING VIA LOCALIZED STATES

In the context of electrical spin injection from ferromagnetic tunnel contacts into semiconductors by local (e.g., three-terminal) detection techniques, it has been proposed that tunneling via localized states in the tunnel contact may, under the right conditions, produce a strongly enhanced spin voltage in a Hanle measurement [41–44]. It is then natural to ask whether or not this can explain the relative strength of electrical and thermal spin currents as observed here. First, we consider the model introduced by Tran *et al.* [41] involving spin accumulation in localized states at or near the insulator/semiconductor interface. Based on the observed scaling of the spin signals with barrier thickness [45], it was already shown that this mechanism cannot be responsible for the large spin voltages observed upon electrical spin injection in ferromagnetic tunnel contacts on semiconductors. Since similar tunnel contacts are used in the present paper, we can rule out this mechanism. Next, we consider the possibility of spin accumulation in localized states in the tunnel barrier itself [42]. For this scenario, the mathematical results of the model by Tran *et al.* [41] still apply; however, the parameters have different meanings, and the scaling with tunnel barrier thickness is different. Experiments reveal that this can indeed create large Hanle spin signals but only if the tunnel barriers are intentionally fabricated in such a way that the barrier is oxygen deficient and/or if unoxidized metal (e.g., Al) remains [43]. In contrast, in devices with properly oxidized tunnel barriers created by plasma oxidation, spin signals due to localized states within the tunnel barrier are absent [45]. Finally, we point out that even if an enhancement of the spin signal due to spin accumulation in localized states in the tunnel barrier or at the barrier/semiconductor interface would be present, it would not affect the comparison made here since our measurement procedure is based on the compensation point. Electrical spin transport by two-step tunneling via localized states produces a spin voltage that is enhanced by the ratio $r_S^{\text{eff}}/r_S^{ch}$ of the effective spin resistance r_S^{eff} of the localized states and the spin resistance r_S^{ch} of the semiconductor channel [41,46]. However, it can easily be shown that a thermally driven spin accumulation in those same localized states will produce a signal enhancement by *exactly the same factor* of $r_S^{\text{eff}}/r_S^{ch}$. Hence, two-step tunneling and spin accumulation in localized states in the tunnel barrier or at the barrier/semiconductor interface does not change the relative strength of thermal and electrical spin currents. The enhancement factor, which is common to both, does not affect the compensation point. Finally, we note that the signal enhancement mechanism recently proposed by Song and Dery [44] relies on the assumption that the energy of the tunneling electrons is much larger than their thermal energy, a condition that does not apply to spin currents that are thermally driven without a net charge tunnel current.

---

[1] A. Fert, Rev. Mod. Phys. **80**, 1517 (2008).

[2] I. Žutić, J. Fabian, and S. Das Sarma, Rev. Mod. Phys. **76**, 323 (2004).

[3] A. Brataas, A. D. Kent, and H. Ohno, Nature Mater. **11**, 372 (2012).

[4] R. Jansen, Nature Mater. **11**, 400 (2012).

[5] T. Jungwirth, J. Wunderlich, and K. Olejník, Nature Mater. **11**, 382 (2012).

[6] G. E. W. Bauer, E. Saitoh, and B. J. van Wees, Nature Mater. **11**, 391 (2012).

[7] A. Slachter, F. L. Bakker, J-P. Adam, and B. J. van Wees, Nature Phys. **6**, 879 (2010).

[8] J. Flipse, F. L. Bakker, A. Slachter, F. K. Dejene, and B. J. van Wees, Nature Nanotech. **7**, 166 (2012).

[9] J. C. Le Breton, S. Sharma, H. Saito, S. Yuasa, and R. Jansen, Nature **475**, 82 (2011).

[10] A. Jain, C. Vergnaud, J. Peiro, J. C. Le Breton, E. Prestat, L. Louahadj, C. Portemont, C. Ducruet, V. Baltz, A. Marty, A. Barski, P. Bayle-Guillemaud, L. Vila, J.-P. Attané, E. Augendre, H. Jaffrès, J.-M. George, and M. Jamet, Appl. Phys. Lett. **101**, 022402 (2012).

[11] K. R. Jeon, B. C. Min, S. Y. Park, K. D. Lee, H. S. Song, Y. H. Park, Y. H. Jo, and S. C. Shin, Sci. Rep. **2**, 962 (2012).

[12] K. R. Jeon, B. C. Min, A. Spiesser, H. Saito, S. C. Shin, S. Yuasa, and R. Jansen, Nature Mater. **13**, 360 (2014).

[13] M. Walter, J. Walowski, V. Zbarsky, M. Münzenberg, M. Schäfers, D. Ebke, G. Reiss, A. Thomas, P. Peretzki, M. Seibt, J. S. Moodera, M. Czerner, M. Bachmann, and C. Heiliger, Nature Mater. **10**, 742 (2011).

[14] N. Liebing, S. Serrano-Guisan, K. Rott, G. Reiss, J. Langer, B. Ocker, and H. W. Schumacher, Phys. Rev. Lett. **107**, 177201 (2011).

[15] W. Lin, M. Hehn, L. Chaput, B. Negulescu, S. Andrieu, F. Montaigne, and S. Mangin, Nature Commun. **3**, 744 (2012).

[16] Ts. Naydenova, P. Dürrenfeld, K. Tavakoli, N. Pégard, L. Ebel, K. Pappert, K. Brunner, C. Gould, and L. W. Molenkamp, Phys. Rev. Lett. **107**, 197201 (2011).

[17] Z. H. Zhang, Y. S. Gui, L. Fu, X. L. Fan, J. W. Cao, D. S. Xue, P. P. Freitas, D. Houssameddine, S. Hemour, K. Wu, and C.-M. Hu, Phys. Rev. Lett. **109**, 037206 (2012).

[18] J. M. Teixeira, J. D. Costa, J. Ventura, M. P. Fernandez-Garcia, J. Azevedo, J. P. Araujo, J. B. Sousa, P. Wisniowski, S. Cardoso, and P. P. Freitas, Appl. Phys. Lett. **102**, 212413 (2013).

[19] S. Hu and T. Kimura, Phys. Rev. B **90**, 134412 (2014).

[20] S. Hu, H. Itoh, and T. Kimura, NPG Asia Mater. **6**, e127 (2014).

[21] P. M. Tedrow and R. Meservey, Phys. Rev. Lett. **26**, 192 (1971).

[22] B. Scharf, A. Matos-Abiague, I. Žutić, and J. Fabian, Phys. Rev. B **85**, 085208 (2012).

[23] R. Jansen, A. M. Deac, H. Saito, and S. Yuasa, Phys. Rev. B **85**, 094401 (2012).

[24] A. Pushp, T. Phung, C. Rettner, B. P. Hughes, S. H. Yang, and S. S. P. Parkin, PNAS **112**, 6585 (2015).

[25] K. R. Jeon, B. C. Min, Y. H. Park, S. Y. Park, and S. C. Shin, Phys. Rev. B **87**, 195311 (2013).

[26] M. Johnson and R. H. Silsbee, Phys. Rev. Lett. **55**, 1790 (1985).

[27] X. Lou, C. Adelmann, M. Furis, S. A. Crooker, C. J. Palmstrøm, and P. A. Crowell, Phys. Rev. Lett. **96**, 176603 (2006).

[28] S. P. Dash, S. Sharma, R. S. Patel, M. P. de Jong, and R. Jansen, Nature **462**, 491 (2009).

[29] S. P. Dash, S. Sharma, J. C. Le Breton, J. Peiro, H. Jaffrès, J.-M. George, A. Lemaître, and R. Jansen, Phys. Rev. B **84**, 054410 (2011).

[30] S. Sharma, S. P. Dash, H. Saito, S. Yuasa, B. J. van Wees, and R. Jansen, Phys. Rev. B **86**, 165308 (2012).

[31] K. R. Jeon, H. Saito, S. Yuasa, and R. Jansen, Phys. Rev. B **91**, 155305 (2015).

[32] S. S. P. Parkin, C. Kaiser, A. Panchula, P. M. Rice, B. Hughes, M. Samant, and S. H. Yang, Nature Mater. **3**, 862 (2004).

[33] S. Yuasa, T. Nagahama, A. Fukushima, Y. Suzuki, and K. Ando, Nature Mater. **3**, 868 (2004).

[34] C. Leavens and G. Aers, Solid State Commun. **61**, 289 (1987).

[35] J. Marschall and A. Majumdar, J. Appl. Phys. **74**, 4000 (1993).

[36] M. Czerner, M. Bachmann, and C. Heiliger, Phys. Rev. B **83**, 132405 (2011).

[37] S.-M. Lee and David G. Cahill, Microscale Thermophys. Eng. **1**, 47 (1997).

[38] S. M. Lee, D. G. Cahill, and T. H. Allen, Phys. Rev. B **52**, 253 (1995).

[39] F. K. Dejene, J. Flipse, G. E. W. Bauer, and B. J. van Wees, Nat. Phys. **9**, 636 (2013).

[40] I. J. Vera-Marun, B. J. van Wees, and R. Jansen, Phys. Rev. Lett. **112**, 056602 (2014).

[41] M. Tran, H. Jaffrès, C. Deranlot, J.-M. George, A. Fert, A. Miard, and A. Lemaître, Phys. Rev. Lett. **102**, 036601 (2009).

[42] O. Txoperena, M. Gobbi, A. Bedoya-Pinto, F. Golmar, X. Sun, L. E. Hueso, and F. Casanova, Appl. Phys. Lett. **102**, 192406 (2013).

[43] O. Txoperena, Y. Song, L. Qing, M. Gobbi, L. E. Hueso, H. Dery, and F. Casanova, Phys. Rev. Lett. **113**, 146601 (2014).

[44] Y. Song and H. Dery, Phys. Rev. Lett. **113**, 047205 (2014).

[45] S. Sharma, A. Spiesser, S. P. Dash, S. Iba, S. Watanabe, B. J. van Wees, H. Saito, S. Yuasa, and R. Jansen, Phys. Rev. B **89**, 075301 (2014).

[46] R. Jansen, S. P. Dash, S. Sharma, and B. C. Min, Semicond. Sci. Technol. **27**, 083001 (2012).